FAST ETCHING OF AMORPHOUS AND MICROCRYSTALLINE SILICON BY HOT-FILAMENT GENERATED ATOMIC HYDROGEN

H.N. WANKA AND M.B. SCHUBERT
University Stuttgart, Institut für Physikalische Elektronik, Pfaffenwaldring 47, D-70569 Stuttgart, Germany

ABSTRACT

A hot tungsten wire effectively dissociates H_2 into atomic hydrogen and thereby facilitates etching and hydrogenation of silicon. Hot filament generated atomic hydrogen etches amorphous silicon (a-Si:H) at a rate of up to 27 Å/s and microcrystalline (µc) Si at rates up to 20 Å/s. A large laminar gas flow is the key to high etch rates. It provides for a fast transport of the etch products out of the reaction zone and thereby avoids redeposition. The etch rate increases with pressure and with H_2 gas flow. Likewise, the etch rate rises with the filament temperature and saturates at a filament temperature of approximately 2150°C when approaching the maximum H_2 dissociation probability. The decrease of the etch rate at higher substrate temperatures is attributed to the loss of the surface coverage by atomic hydrogen. The etch selectivity between a-Si:H and µc-Si drops at elevated substrate temperatures. Boron doping decreases the etch rates both for a-Si:H and µc-Si, whereas phosphorous doping does not significantly affect it. This etch selectivity is caused by a catalytic effect of BH_3 on the surface hindering the formation of the main etch product silane. Even for highest etch rates no surface roughening of a-Si:H occurs, however, a bond structure modification of the near surfaces arises, an effect which results in the formation of a nanocrystalline surface layer. The increase of the µc-Si etch rate close to the film substrate interface characterizes the film thickness at which the coalescence of the microcrystalline nuclei starts.

INTRODUCTION

Etching is one of the most important processing steps in large area microelectronics, especially in the fabrication of integrated circuits. Until now, silicon is the most employed element in semiconductor technology, be it as crystalline (c-Si), microcrystalline (µc-Si), and amorphous hydrogenated (a-Si:H). Several wet and dry etching processes are available for Si [1-4]. The gases CF_4 or CCl_4 and mixtures with O_2 are commonly used as dry etching gases. Since the Si etch rate depends on the doping level [5] and the material structure (a-Si:H is etched faster than µc-Si [6] and in turn µc-Si faster than c-Si [2]) etch selectivity is ensured. Thereby etch stops and self-aligning etching are feasible. Etching by hydrogen ions or radicals [7,8] is a very interesting application, especially, if halogens are to be avoided and for hydrogen is one of the Si processing involved gases.

In the recent years there is growing interest in the hot filament chemical vapor deposition of amorphous [9,10] and microcrystalline Si [11-13] since high growth rates are achieved at a reasonable material quality. A hot tungsten surface effectively dissociates SiH_4 [14] and H_2 [15,16]. However, there have been only a few studies investigating the interactions of hot filament generated atomic hydrogen (HFGAH) with bulk silicon. An et

Mat. Res. Soc. Symp. Proc. Vol. 467 © 1997 Materials Research Society

al. [17] reported a-Si:H etching by HFGAH at a rate of 0.17 Å/s without surface roughening, whereas Nguyen and coworkers [18] showed that a thin microcrystalline surface layer is riding on the etch front which likewise moves at 0.17 Å/s. In this study, we demonstrate that high etch rates of a-Si:H and μc-Si are achieved by HFGAH etching and we show the application to etch selectivity.

EXPERIMENTAL

A high vacuum system equipped with a molecular drag pump is used for the growth and etching of the a-Si:H and μc-Si films. Hot-wire chemical vapor deposition (HWCVD) serves to deposit a-Si:H films at a substrate temperature of 400°C, at a pressure of 2.5 Pa and a SiH_4 gas flow of 9 sccm. A 250 μm thick and 4 cm long single tungsten wire at a temperature of 1650°C, at a substrate to filament distance of 2 cm results in a growth rate of 20 Å/s. These deposition conditions yield device quality a-Si:H with a hydrogen content of 3% [10]. The μc-Si films are grown by applying the following parameters: $[H_2]/[SiH_4]$ dilution ratio 30, H_2 flow 60 sccm, pressure 15 Pa, and filament temperature 1750°C. As standard etch conditions we use a filament temperature of 1850°C, a H_2 flow of 80 sccm, a pressure of 20 Pa, and a substrate temperature of 400°C. Special care is taken to maintain a laminar gas flow in the reactor. The distance of the sample holder and the filament to the reactor walls is more than 10 cm. Thereby, the influence of the reactor walls is reduced. A phase-modulated in-situ ellipsometer (Jobin-Yvon, UVISEL) monitors the growth and etching of the films to determine the rates. Kinetic measurements (as fast as 100 ms per data point) are carried out at a photon energy of 4 eV, for highest surface sensitivity. In addition to HWCVD grown samples, a-Si:H films from plasma-enhanced chemical vapor deposition (PECVD) were under investigation for etch experiments. During transfer of these samples the vacuum had to be broken resulting in a slight surface oxidation. Taking the removal of the native oxide into account, the PECVD films exhibit comparable etch rates as the HWCVD a-Si:H films, which is in agreement with recent findings [8] on the a-Si:H hydrogen etch rate being insensitive to the material structure.

RESULTS AND DISCUSSION

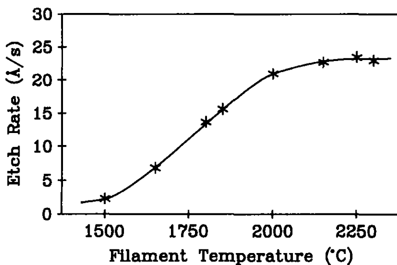

Fig. 1: The dependence of the a-Si:H etch rate on the filament temperature

Figure 1 shows the increase of the a-Si:H HFGAH etch rate with the filament temperature and besides that unchanged standard etch conditions. This increase is in accordance with a pronounced H generation at the filament at higher temperatures. The a-Si:H etch rate saturates at approximately 22 Å/s at a filament temperature of about 2150°C. This observation is attributed to a saturation of the H_2 dissociation probability at 30% at the filament [16] which is caused by a drop of the H_2 sticking probability at elevated tungsten temperatures.

The main key to achieve high HFGAH etch rates is the generation of a large amount of atomic hydrogen in combination with a short dwell-time of the species in the etch system. Etching is more pronounced than deposition which

occurs simultaneously since the main etch product silane [19] may be decomposed at the hot filament. A fast transport of the etch products out of the reactor, which is achieved by a high hydrogen flow as demonstrated in Fig. 2 (a), reduces the redeposition probability. We interpret the decrease of the etch rate with decreasing H_2 flow as a result of loading the reactor with silane. In Fig. 2 (b) the effect of the pressure on the etch rate is shown at a H_2 flow of 10 sccm. In this pressure regime an increase of the pressure results in a linear increase of the etch rate. This result is comparable to the findings of Vepřek and Sarott [7] on silicon etching by a hydrogen low-pressure plasma. However, we find no silicon deposition on the samples at low pressure and low hydrogen flow which may be caused by chemical transport [20].

A decrease of the c-Si etch rate at higher substrate temperatures was reported for H_2-plasma etching [21] and for molecular beam etching [19,22]. Otobe et al. [8] found a decrease of the a-Si:H and c-Si etch rate in a very high frequency (VHF) H_2-plasma and a decrease of the etch selectivity between a-Si:H and c-Si at elevated substrate temperatures. A pronounced bulk diffusion of absorbed atomic hydrogen at elevated substrate temperatures [19], a decrease of the surface coverage of chemisorbed atomic hydrogen due to recombination [7] or a more temperature activated desorption of atomic hydrogen than bond breaking [8] were proposed for explanation.

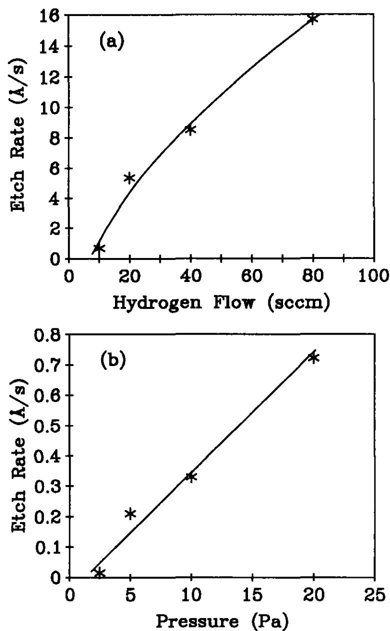

Fig. 2: The dependence of the a-Si:H etch rate on the H_2 gas flow (a) at a pressure of 20 Pa and on the pressure (b) at a H_2 gas flow of 10 sccm (substrate temperature 400°C).

Figure 3 shows the drop of the HFGAH etch rate at higher a-Si:H and μc-Si substrate temperatures at a pressure of 20 Pa and H_2 gas flow of 80 sccm. This effect is similar to the etching of c-Si by other atomic hydrogen etch techniques. The etch selectivity between a-Si:H and μc-Si increases from 1.3 to 3.9 from 25° to 400°C substrate temperature. This finding is different from the a-Si:H and c-Si H_2 VHF etch plasma results of Otobe et al. [8]. Their findings may, however, have been masked by chemical transport of Si from the counter electrode to the substrate, an effect which is pronounced at higher substrate temperatures [21]. Since the nucleation of μc-Si is more favorable on crystalline substrates than on amorphous ones [6], the decrease in effective c-Si etch rates with temperature found by Otobe et al. [8] is lower than

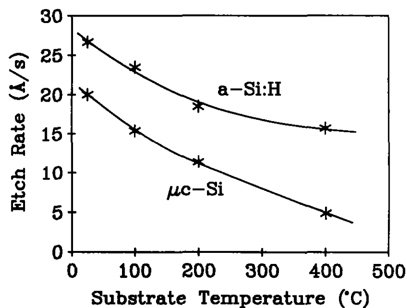

Fig. 3: Decrease of the a-Si:H and μc-Si etch rates at elevated substrate temperatures

expected from our data. Our findings suggest that the decrease of the Si etch rate at elevated temperatures is caused by a combination of hydrogen losses by diffusion into the bulk, which exhibits a higher activation energy in c-Si than in a-Si:H [23,24] and by hydrogen desorption into the gas phase. We did not find a significant dependence of the μc-Si etch rate on the grain size, which can be varied via the hydrogen dilution ratio during deposition [13].

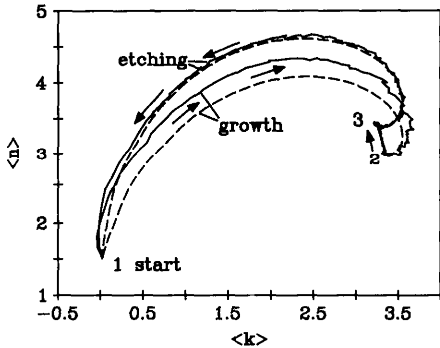

Fig. 4: in-situ ellipsometry, growth and etching of a-Si:H (photonenergy 4 eV). Bond structure modification in the first 5 s (2→3). Data remain stable (3) since transparency is achieved.

Figure 4 presents in-situ ellipsometry trajectories in the pseudo refractive index <n> and the pseudo extinction coefficient <k> plane of the growth and etching of HWCVD a-Si:H on a glass substrate at standard conditions. The dashed lines refer to the modelling of homogeneous growth and etching. The trajectory starts at the optical data of the substrate (1). The deviations of the measurement from the simulation occur during growth due to a-Si:H nucleation and filling up of the surface roughness of the substrate. The growing film becomes opaque at a film thickness of about 30 nm and the trajectory settles in point (2). When etching is started, the measured data move from (2) to (3) in the first 5 s and then remain stable in (3) until transparency is reached again. During etching of the last 30 nm of film thickness, the ellisometry data move from (3) to (1). The shift of the measured data from (2) to (3) corresponds to 8 nm a-Si:H etching and translates in a blue shift of spectroscopic ellipsometry data. This blue shift or movement of the single wavelength ellipsometry data can be modelled assuming the formation of a three monolayer thick porous nanocrystalline surface layer and the incorporation of additional hydrogen in the near surface bulk a-Si:H. This bond structure relaxation due to the impact of atomic hydrogen is known from H_2-plasma treatments, which form a thin crystalline surface layer on a-Si:H [25] and were also found by Nguyen and coworkers [18] during a-Si:H etching by hot filament generated atomic hydrogen at a rate of 0.17 Å/s. It is remarkable, that the formation of this nanocrystalline surface layer even occurs at our etch rates which are more than two orders in magnitude higher. Transmission electron microscopy (TEM) exhibited a grain size of approximately 2-4 nm at 20 % crystalline phase [26] of this surface layer. Additionally TEM shows a doubling of the void size in the amorphous bulk. During a-Si:H etching at 250°C substrate temperature, the blue shift of spectroscopic ellipsometry data is less distinct and disappears at room temperature etching. Therefore, during room temperature etching, no nanocrystalline surface layer is formed. At 400°C after the formation of the nanocrystalline surface layer, which is riding on the etch front, the ellipsometry data remain stable (2). Consequently, the HFGAH etching of a-Si:H occurs homogeneously on a monolayer scale without surface roughening independent of the etch process parameters. In contrast to a-Si:H etching the surface roughness of μc-Si increases with etch depth, due to different surface stability of the various crystal orientations of the grains.

In halogen containing etch plasmas, n-type Si etches faster than undoped Si and in turn intrinsic Si faster than p-type material [1,2,5]. A Fermi level dependent chemisorbtion of the halgones was proposed for explanation [5]. HFGAH etching of a-Si:H and μc-Si exhibits a

decrease of the rates for boron doped material, whereas phosphorous doping does not affect it. The doping concentrations in Fig. 5 are given as gas phase dilution ratios $[B_2H_6]/[SiH_4]$ and $[PH_3]/[SiH_4]$. The increase in etch selectivity between a-Si:H and μc-Si for B-doped films is probably caused by an enhanced B incorporation in HWCVD μc-Si as compared to HWCVD a-Si:H. Adding $[B_2H_6]$ in the gas phase during a-Si:H deposition results in an increase of the growth rate due hydroboron radicals on the surface which catalyze H_2 desorption [27]. In our opinion the same catalytic effect occurs in the case of etching: hydroboron radicals, which have a low surface loss probability, accumulate at the etch front. Thereby hydrogen depletion of the etch front occurs which results in a decrease of the etch rate. In contrast to n-type and intrinsic Si, etching of *boron doped* Si by atomic hydrogen changes the surface chemistry. We suggest that this doping dependent etch selectivity is common to all atomic hydrogen etch techniques, when applied to silicon.

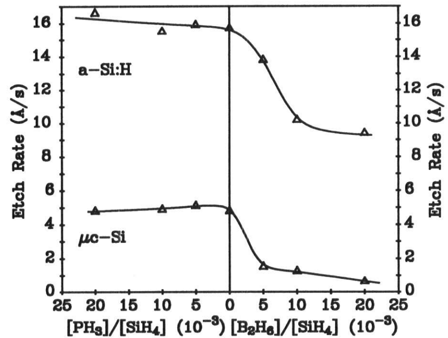

Fig. 5: a-Si:H and μc-Si etch rates as functions of doping at standard etch conditions

Metals and SiO_2 are not etched by HFGAH. Figure 6 shows a simple, however, useful application of this etch technique, the etching of a-Si:H solar cells between the metal contacts on a ZnO substrate. No underetching of the Al contact occurs and the crosstalk of the cells due to the doped layers is removed in a fast and easy way. This technique has no detrimental effects on the cells, even on a SnO_2 substrate, when etching is performed at room temperature. Another nice application of hot filament generated H is to detect the film thickness where μc-Si nuclei come into contact. Boron-doped μc-Si HWCVD films have been etched and the rate has been monitored over film thickness. The rate is constant down to a film thickness of approximately 20 nm and then begins to increase by about a factor of 2 to 3 due to the interface porosity of the μc-Si film. This onset of the increase in etch rate reflects the initial coalescence of the μc-Si nuclei. In addition to Si etching HFGAH facilitates a powerful method for hydrogenation of μc-Si and polycrystalline Si. The photo to darkconductivity ratio of HWCVD μc-Si has been improved from 10 to 200 in a treatment time of 30 min at conditions of weak etching. Additionally, the diffusion length in polycrystalline Si and thereby cell efficiency were improved in an impressive way [28].

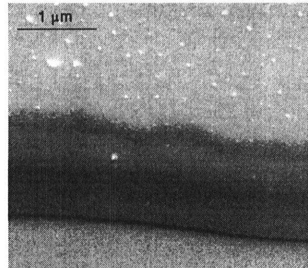

Fig. 6: Etch edge of Al on a-Si:H on a ZnO substrate

CONCLUSION

Apart from etching Si, HFGAH represents a powerful technique for Si hydrogen passivation and has a high potential for industrial application. The etch rate is mainly controlled by a fast transport of the etchants out of the reactor and the generation of a large amount of atomic

hydrogen. This technique facilitates etch selectivity, since SiO_2 and metals are not etched. The surface damage of this technique is neglectable because the process is controlled by surface chemistry and no accelerated species hit the surface. Boron dopants change the surface chemistry, reduce the surface hydrogen coverage and thereby the etch rate. Etching of a-Si:H starts with the formation of a thin nanocrystalline surface layer, which rides even at highest rates on the etch front. However, this network relaxation is etch rate independent controlled by the substrate temperature.

ACKNOWLEDGEMENTS

The authors wish to thank M. Albrecht and S. Aldabergenova at the University of Erlangen for TEM analyses and the German BMBF for financial support under contract nos. 0329521A and 0329634 .

REFERENCES

1. C.A. Desmond, C. E. Hunt, and S.N. Farrens, J. Electrochem. Soc. **141**, 178 (1994).
2. I. Haller, Y.H. Lee, J.J. Nocera, Jr., and M.A. Jaso, J. Electrochem. Soc.: Solid-State Science and Technology **135**, 2042 (1988).
3. Y. Okada and S. Wagner, Mat. Res. Soc. Symp. Proc. **192**, 541 (1990).
4. P.E. Clarke, D. Field, and D.F. Klemperer, J. Appl. Phys. **67**, 1525 (1990).
5. L. Baldi and D. Beardo, J. Appl. Phys. **57**, 2221 (1985).
6. W. Westlake and M. Heintze, J. Appl. Phys. **77**, 879 (1995).
7. S. Vepřek and F.-A. Sarott, Plasma Chemistry and Plasma Processing **2**, 233 (1982).
8. M. Otobe, M. Kimura, and S. Oda, Jpn. J. Appl. Phys. **33**, 4442 (1994).
9. A.H Mahan, J. Carapella, B.P. Nelson, R.S. Crandall, and I. Balberg, J. Appl. Phys. **69**, 6728 (1991).
10. M. Heintze, R. Zedlitz, H.N. Wanka, and M.B. Schubert, J. Appl. Phys. **79**, 2699 (1996).
11. J. Cifre, J. Bertomeu, J. Puigdollers, M.C. Polo, J. Andreu, and A. Lloret, Appl. Phys. A **59**, 645 (1994).
12. A.R. Middya, J. Guillet, J. Perrin, and J.E. Bouree, Mat. Res. Soc. Symp. Proc. **420**, 289 (1996).
13. H.N. Wanka, R. Zedlitz, M. Heintze, and M.B. Schubert, Mat. Res. Soc. Symp. Proc. **420**, 295 (1996).
14. H. Wiesmann, A.K. Ghosh, T. McMahon, and M. Strongin, J. Appl. Phys. **50**, 3752 (1979).
15. I. Langmuir, J. Am. Chem. Soc. **34**, 1310 (1912).
16. J.N. Smith Jr. and W.L. Fite, J. Chem. Phys. **37**, 898 (1962).
17. I. An, Y.M. Li, C.R. Wronski, and R.W. Collins, Phys. Rev. B **48**, 4464 (1993).
18. H.V. Nguyen, I. An, R.W. Collins, Y. Lu, M. Wakagi, and C.R. Wronski, Appl. Phys. Lett. **65**, 3335 (1994).
19. J. Abrefah und D.R. Olander, Surf. Sci. **209**, 291 (1989).
20. S. Vepřek and V. Mareček, Solid State Electron. **11**, 683 (1968).
21. A.P. Webb and S. Vepřek, Chem. Phys. Lett. **62**, 173 (1979).
22. S.M. Gates, R.R. Kunz, and C.M Greenlief, Surf. Sci. **207**, 364 (1989).
23. S.J. Pearton, J.W. Corbett, and T.S. Shi, Appl. Phys. A **43**, 153 (1987).
24. P.V. Santos and W.B. Jackson, Phys. Rev. B **46**, 4595 (1992).
25. H. Shirai, B. Drévillon, and I Shimizu, Jpn. J. Appl. Phys. **33** Part 1, 5590 (1994).
26. H.N. Wanka, S. Aldabergenova, M. Albrecht, and M.B. Schubert, unpublished.
27. J. Perrin, Y. Takeda, N. Hirano, Y. Takeuchi, and A. Matsuda, Surf. Sci. **210**, 114 (1989).
28. R. Plieninger, H.N. Wanka, J. Kühnle, and J.H. Werner, unpublished.